Experimental Propeller Performance Characterisation behind a Towed Axisymmetric Body

Alexander Conway, DST Group, Australian Maritime College,
alexander.conway@dst.defence.gov.au
Chetan Kumar, DST Group, chetan.kumar@dst.defence.gov.au
Anthony Fowler, DST Group, RMIT University, anthony.fowler@dst.defence.gov.au
Rudaba Khan, DST Group, rudaba.khan@dst.defence.gov.au
Adam Rolls, Australian Maritime College, adam.rolls@utas.edu.au

ABSTRACT

The performance of a marine propeller is degraded by non-ideal operating conditions, including environmental disturbances and vehicle motion. A closed-loop controller can help to overcome these effects and maintain performance. As control law design and implementation requires a model of the system, the propeller must be characterised. To this effect, the performance of a propeller operating behind a towed axisymmetric body was captured via an experimental investigation at the Australian Maritime College (AMC) towing tank. All tests were performed on a generic underwater vehicle geometry with a generic 5-bladed propeller.

All experiments were undertaken with the model straight-ahead and deeply submerged. Computational Fluid Dynamics (CFD) and empirical methods were used to estimate the wake deduction factor to calculate the speed of advance.

The measured thrust, torque and efficiency curves were compared to open-water propeller curves undertaken on the same propeller geometry at the AMC Cavitation tunnel. Differences in experimental setup compared to the cavitation tunnel were accounted for using the ITTC guidelines regarding Reynolds independence. The carriage velocity and propeller rotational speeds were selected to ensure the same flow regime between both data sets.

The results indicate that the open-water propeller curves can provide reasonable estimates of propeller performance in straight-line, deeply submerged condition, provided the wake deduction factor is accurately estimated.

This data will be used to demonstrate real-time closed-loop thrust control techniques in future experimental trials. Further work will investigate the impact of model yaw and aft-control surface deflections on propeller performance.

INTRODUCTION

Marine vehicle propulsion systems often operate in far from ideal conditions that can result in significant thrust losses. These may result from the environmental state, vehicle motion, interactions between the vehicle and propeller and ventilation, which occurs when surface air or exhaust gases are drawn into the propeller blades due to a decrease in pressure [1]. In addition to potentially increasing the mechanical wear on the propulsion system, these thrust losses are detrimental to the manoeuvring performance of the vehicle.

The implementation of a closed-loop feedback control system to compensate for the losses in thrust performance can improve overall propeller performance in maritime applications [2]. By measuring relevant outputs from the propulsion system in real time, an appropriately designed control law can respond to disturbances acting on the propulsion system to maintain the desired propeller behaviour.

To facilitate control law design, a plant model describing the performance of the system to be controlled is necessary. Accurately predicting the thrust and torque generated by a marine propeller often involves the development of complex dynamic models, particularly if an accurate representation of the transient behaviour of the propeller is required [3]. For the purposes of control design, however, it is usually considered sufficient to use simpler empirical models, such as the conventional propeller curves based on non-dimensional thrust and torque coefficients [4].

Open-water experimental tests are commonly performed to characterise a propeller and generate its performance curves [5-7]. However, these curves no longer provide an accurate representation of the propeller's performance once it is placed behind a vehicle due to the resulting changes in flow conditions. For an underwater vehicle, a significant non-uniform wake is created by the hull, casing, sail and aft appendages [8], which leads to a reduction in the flow velocity into the propeller. For the purposes of control law design, it is therefore preferred to obtain a propeller model that captures the actual wake-affected behaviour of the propeller behind the vehicle, rather than in ideal open-water conditions. Thus, the open-water propeller characterisation approaches typically performed and described in the literature are not suitable for this purpose.

This paper describes an experimental study to characterise the performance of a marine propeller. In contrast to conventional open-water experiments, the behaviour of the propeller is assessed while located behind a towed axisymmetric body to generate performance data under realistic flow conditions. For this purpose, a generic geometry underwater body was fitted with the DSTG 115-1 fixed-pitch, 5-blade propeller [9]. Through an experimental program undertaken at the Australian Maritime College (AMC) towing tank, performance curves describing the propeller's non-dimensional thrust, torque and efficiency over the first quadrant of operation were generated. All experiments were undertaken with the model straight-ahead and deeply submerged.

The tests were performed using a newly designed and constructed test model. For verification and comparison purposes, a subset of the captured propeller performance data was compared to existing performance curves generated via open-water tests on the same

propeller at the AMC cavitation tunnel [10]. To compensate for the effect of operating in the wake of the test model, Computational Fluid Dynamics (CFD) and empirical methods were used to estimate the wake deduction factor to calculate the actual speed of advance, allowing direct comparisons to be made between the data sets.

EXPERIMENTAL SETUP

The underwater vehicle model used in this study is a modified version of the Defence Science and Technology (DST) Group Joubert barehull model with aft control surfaces [11]. The axisymmetric model has a diameter of 0.3 m and a fixed length (L) of 1.3 m, resulting in a length to diameter (L/D) ratio of 4.33. It is axisymmetric for the first 0.07L from the nose tip, with the nose derived from a NACA-0018 forebody. The body is axisymmetric with a fared sail (NACA-0022) and X-form aft control surfaces. The model uses a 5-blade DST generic submarine propeller (shown in Figure 1) with a diameter of 0.15 m, located at 0.98L. Details of the propeller are given in Table 1. For details on the X-form geometry, see Joubert [11] and Overpelt [12]. The model was mounted via a streamlined sail-shaped holding strut, as shown in the schematic drawing of the experiment model in Figure 2.

Figure 1 - DSTG 115-1 propeller with 0.15 m diameter.

Table 1 - Properties of DSTG 115-1 propeller used in the experiments [10].

Description	**Value**
Diameter	0.15 m
Number of blades	5
Expanded blade area ratio	0.60
Pitch ratio	1.20
Skew angle	44.5°

The tests were carried out at a submergence centreline depth of approximately 0.671 m, which is mid-depth in the towing tank. This ensures that the surface and bottom effects are minimised. The propeller diameter was sized to maximise thrust and torque measurements whilst minimising its free-surface impact. All measurements were carried out at approximately zero angles of yaw and pitch, with the accuracy for setting yaw and pitch being approximately 0.1°. The origin of the body coordinate system is located at the nose of the model.

The model was tested in the 100 m AMC towing tank [13] at freestream velocities from 2.25 m/s to 3.95 m/s, which correspond to propeller Reynolds numbers of 2.02×10^5 to 2.22×10^5 for the validation cases.

The propeller Reynolds number is given by:

$$Re_P = \frac{v_{res} c_{0.7D}}{\nu} \tag{1}$$

where

$$v_{res} = \sqrt{v_a^2 + (0.7\pi D n)^2} \tag{2}$$

and Re_P is the propeller Reynolds number, v_{res} is the velocity of the blade at $0.7D$, $c_{0.7D}$ is the blade chord length at $0.7D$, ν is the kinematic viscosity, v_a is the speed of advance of the propeller, D is the propeller diameter and n is the revolutions per second of the propeller.

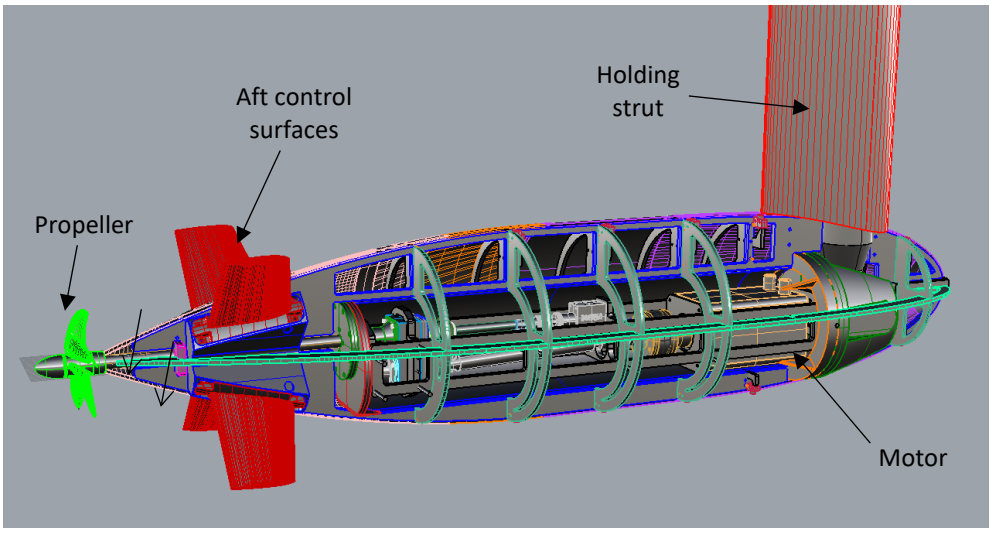

Figure 2 - Schematic drawing showing internal layout and external shape of the experiment model.

Thrust and Torque Measurement

The motor and data acquisition electronics for the thrust and torque measurements were housed inside a waterproof section, as shown in Figure 3. The propeller was driven by an Aerotech BM800 motor, and the propeller thrust and torque were measured using a MARIN 200 N seakeeping dynamometer attached to the propeller. The thrust and torque calibration were checked using a custom designed, in-situ calibration rig. The calibration data indicates a precision of 0.5 N for the thrust and 0.02 Nm for the torque. The total measurement uncertainty based on both systematic and random sources was estimated to be approximately 5% (confidence interval 95%).

Figure 3 - Cross section of the towing tank model with waterproof section.

Hama Strip - Artificial Turbulence Stimulator (ATS)

Due to the size of the model and the carriage speeds required, laminar flow was predicted across the majority of the test cases. In order to allow the propeller to operate in conditions which represent those encountered on a full scale underwater vehicle, turbulence stimulation to generate a turbulent boundary layer was implemented.

The Hama strip consists of a span-wise array of triangular planform protuberances arranged in a repeating pattern. It was proposed by Hama [14] to provide a means of transitioning laminar to turbulent flow with low levels of parasitic drag in towing tank or wind tunnel model testing. The Hama strips were made from PVC electrical tape, with the protuberance edge defined using a pair of 5 mm pinking scissors. The Hama strip was attached to the model circumferentially and located at a streamwise location of x/L = 5%. The Hama strip was also attached to the holding strut and located at x/L = 10%, as shown in Figure 4. The aft-control surfaces were not tripped. The height of the Hama strips was chosen to be approximately 1 mm to ensure the flow remained turbulent across the test speed range. The trip height was sized based on previous studies in the towing tank, as discussed in Kumar [13].

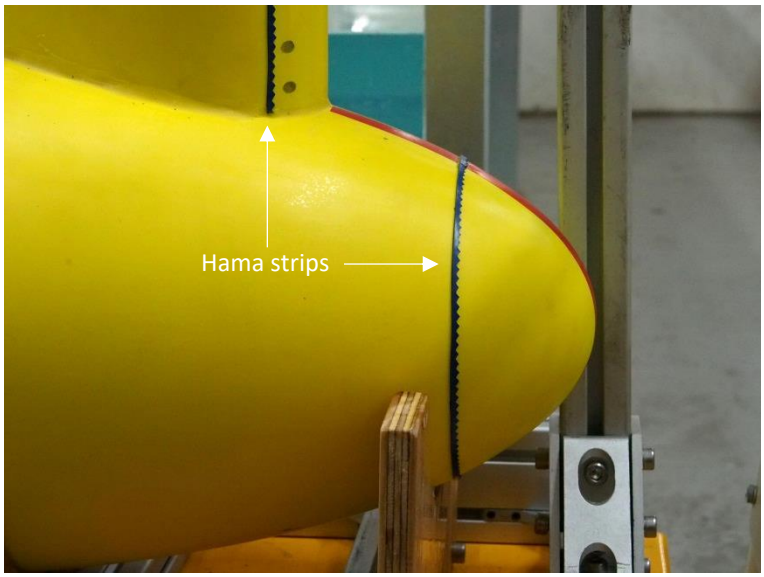

Figure 4 - Placement of Hama strip at the nose (x/L = 5%) and the sail (x/L = 10%).

VELOCITY OF ADVANCE CALCULATION

A critical factor in determining the thrust and torque coefficients is accurately predicting the speed of advance of the propeller. Therefore, both a numerical and an empirical approach were utilised to assess the velocity of the flow encountered by the propeller behind the axisymmetric body.

Using the empirical approach proposed by Renilson [8], adapted from Burcher and Rydill [15], the empirical Taylor wake fraction was predicted using Figure 5. As the prop/hull ratio for the model is 0.5 and it has a tail cone angle of 20°, the Taylor wake fraction is estimated as 0.31. The equation for Taylor wake fraction is,

$$\omega = \frac{v - v_a}{v} \tag{3}$$

where ω is the Taylor wake fraction and v is the forward speed of the vessel. Rearranging the equation and with a Taylor wake of 0.31 results in a speed of advance as,

$$v_a = 0.69v \tag{4}$$

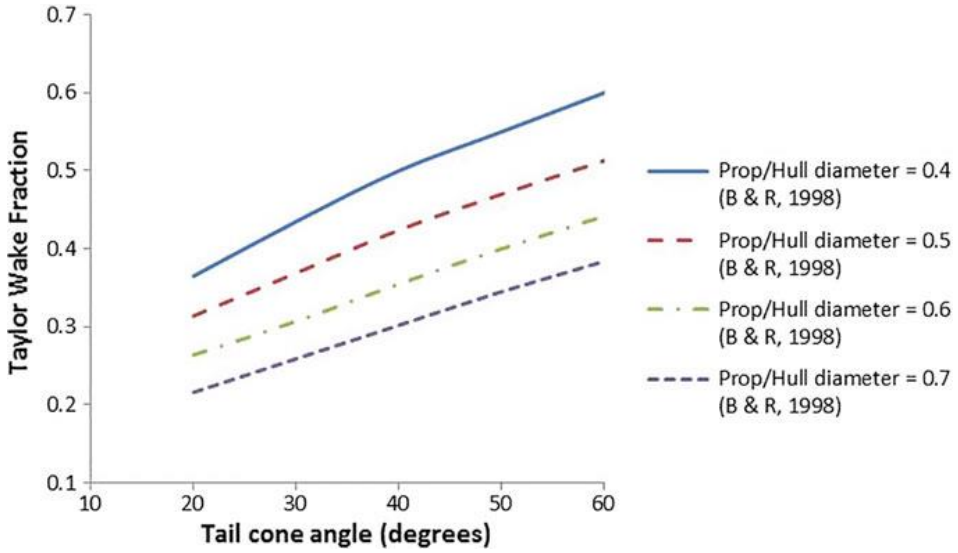

Figure 5 - Taylor wake fraction for underwater vehicles based on prop/hull diameter ratio and tail cone angle [8].

The speed of advance of the propeller was also predicted using CFD. The CFD software *Fluent* was used to perform the numerical simulations with a fully structured mesh generated in *Pointwise*. A grid independence study and validation was completed as discussed previously in Conway [16]. Figure 6 shows the axial velocity contour slice at the propeller plane. The free stream velocity for the simulation was 1.6 m/s and the average velocity was interpolated across the grid at 0.7D, where D is the propeller diameter, as 0.7D is location of maximum chord length [17] and the maximum load on a propeller. The speed of advance was thus calculated as 0.68v.

As both methods provided very similar predictions for the speed of advance, it was decided to use $v_a = 0.68v$, as the validated CFD simulations were assumed to have a higher accuracy than the empirical method.

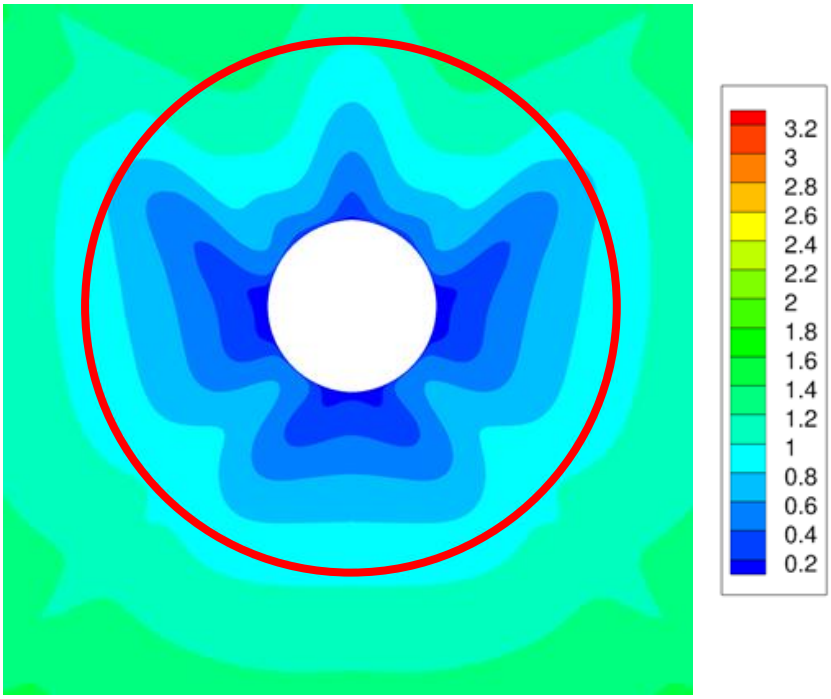

Figure 6 - Axial velocity gradient at the propeller plane for the BB2 submarine with a free stream velocity of 1.6 m/s. The red circle represents 0.7*D* for velocity prediction.

RESULTS/DISCUSSION

Experimental Data Validation

The initial test runs were performed for the non-dimensional advance coefficient (J) values in the range 0.7 to 1.3, with the resulting values for the thrust coefficient (K_T) and torque coefficient (K_Q) being shown in Figure 7. The J value was calculated using equation (7) below. The thrust and torque data is plotted in terms of K_T and K_Q coefficients calculated using equations (5) and (6). The efficiency (η) of the propeller was calculated using equation (8).

$$K_T = \frac{T}{\rho n^2 D^4} \tag{5}$$

$$K_Q = \frac{Q}{\rho n^2 D^5} \tag{6}$$

$$J = \frac{V_a}{nD} \tag{7}$$

$$\eta = \frac{K_T}{K_Q}\frac{J}{2\pi} \tag{8}$$

where T is the thrust, Q is the torque and ρ is the water density.

In order to validate the experimental results generated using the towing tank model, the data was compared to previous experimental data generated in the AMC cavitation tunnel using the same 5-bladed propeller geometry having a diameter of 250 mm in open-water conditions [10]. The propeller rotation rate and carriage speeds were carefully selected to maintain Reynolds independent flow when compared to the experiment conducted in the cavitation tunnel.

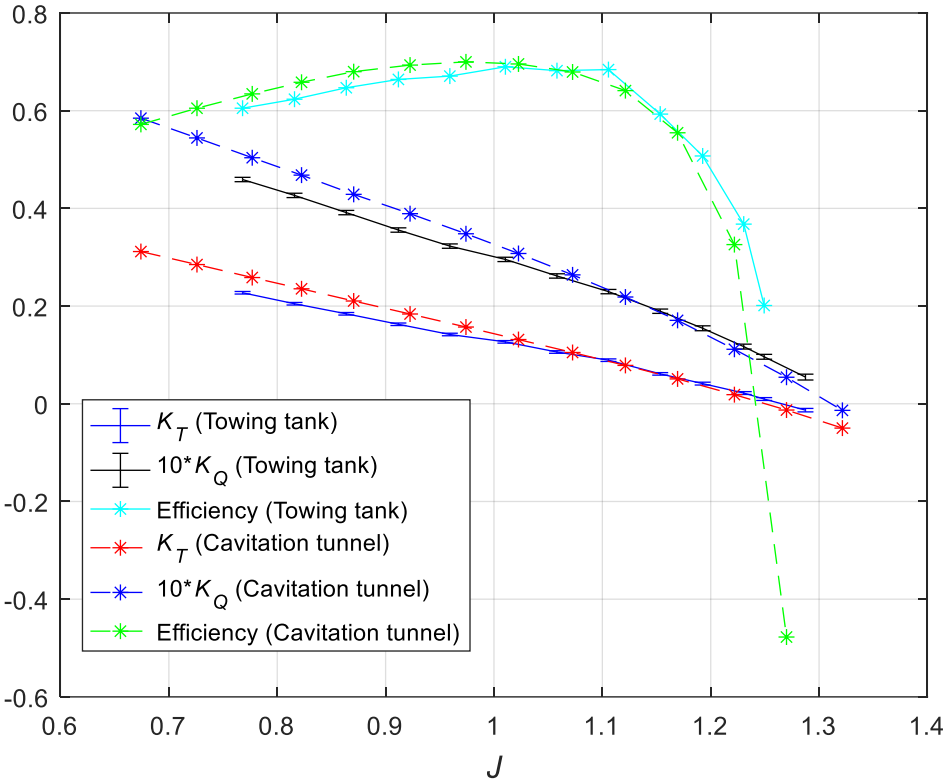

Figure 7 - Efficiency (η), thrust coefficient (K_T) and torque coefficient (K_Q) plotted against advance coefficient (J) values for the towing tank experiment and cavitation tunnel data [10].

As is seen in Figure 7, the correlation between the towing tank and cavitation tunnel data for thrust, torque and efficiency show similar trends, with a slight shift to the right for the towing tank data. Whilst all efforts were made to accurately predict the average inflow velocity of the propeller, as discussed earlier, it is hypothesised that this shift to the right is due to an over estimation in the speed of advance of the propeller by a small margin. However, due to the complex nature of the flow around the mounting strut and aft control surfaces, slight variations between the propeller operating in open water can be expected. Other variations in the data could be due to changes in Reynolds number. Although ITTC procedures suggest that Reynolds independent flow has been achieved, further investigation into the effects of varying Reynolds number would be required to confirm that this has not affected the results published above. A Reynolds dependency study will be conducted during the next phase of experiments.

The strong correlation between the two sets of data suggests that the experimental configuration and dynamometer used are appropriate to accurately capture the full quadrant thrust and torque values accurately.

First Quadrant Propeller Characterisation

For a fixed pitch propeller, it is possible to define four quadrants of operation based on an advance angle β as defined as [4],

$$\beta = \tan^{-1}\left(\frac{v_a}{0.7\pi nD}\right) \tag{9}$$

It is common practice to concentrate on first quadrant operation, where the propeller is spinning in the positive direction with forward advance velocity, as this represents normal operating conditions. However, designing a controller capable of handling all operating conditions ultimately requires characterising all four quadrants of propeller operation, including astern performance [2]. In this case, the use of J, K_T and K_Q when characterising propeller performance becomes mathematically problematic when approaching the quadrant boundaries.

A more flexible approach is to use the alternative non-dimensional thrust coefficient (C_T) and torque coefficients (C_Q) defined in [4] as,

$$C_T = \frac{T}{\left(\frac{\pi}{8}\right)\rho\left[V_a^2+(0.7\pi nD)^2\right]^2} \tag{10}$$

$$C_Q = \frac{Q}{\left(\frac{\pi}{8}\right)\rho\left[V_a^2+(0.7\pi nD)^2\right]^3} \tag{11}$$

These coefficients are well defined across all four operating quadrants (i.e. $0^\circ \leq \beta \leq 360^\circ$) and are therefore suitable for characterising propeller performance for control design and simulation purposes.

Having validated the obtained experimental data for J values in the range of 0.7 ($\beta = 17.7^\circ$) to 1.3 ($\beta = 30.6^\circ$), further propeller thrust and torque measurements were then obtained for the complete first quadrant from $\beta = 0^\circ$ (ahead bollard pull condition) to $\beta = 90^\circ$ (ahead motion with propeller stationary). The resulting propeller performance coefficients C_T and C_Q are plotted versus β in Figure 8. For comparison purposes, this figure also includes first-quadrant propeller data from Pivano et al. [2]. While the comparison data was obtained in open-water conditions and with a different propeller, it is nevertheless useful to compare the trends between the two data sets. The thrust and torque values produced by the propeller tested in this work are smaller at higher values of β, however it is seen that there are similar trends in the performance coefficients, therefore providing further validation for the experimental approach used.

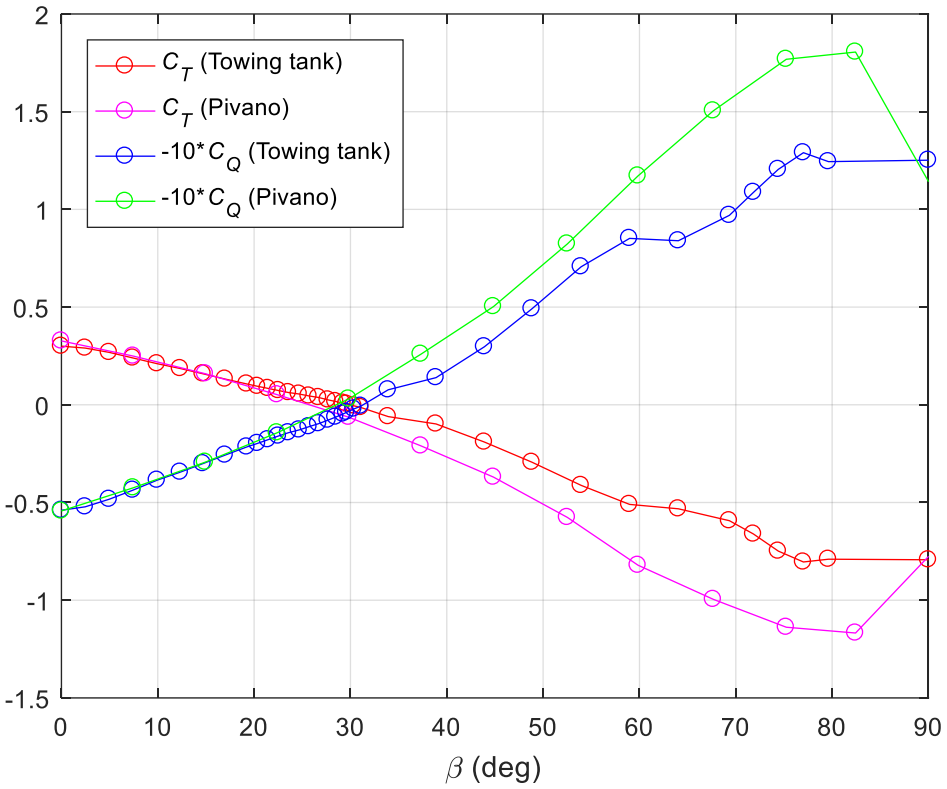

Figure 8 - Experimentally obtained non-dimensional thrust coefficient (C_T) and torque coefficient (C_Q) vs. advance angle (β) for first propeller quadrant. Results compared with data from Pivano [2].

CONCLUSION

The thrust and torque generated by a propeller operating behind an underwater vehicle have been investigated in this paper. Experiments were conducted in the AMC towing tank using a custom-made axisymmetric body with control surfaces. Using the estimated wake deduction factor calculated from CFD, the thrust and torque values recorded in the towing tank were validated against open-water cavitation tunnel data. The validation showed strong correlation between the two sets of data. This was followed by obtaining the propeller characteristics across the complete first quadrant from $\beta = 0^{\circ}$ to $\beta = 90^{\circ}$, providing an initial capability to develop control algorithms for standard operating conditions.

In contrast to the typical open-water experiments that are performed to assess propeller performance, this work allows a realistic propeller model to be generated that incorporates the non-ideal flow effects that arise from operating behind a body. Future work will involve characterising the performance of the propeller in the same manner across the remaining three quadrants involving astern, crashback and crashforward conditions. This will allow the generation of a complete empirical propeller model that will be used in the design of four-quadrant closed-loop thrust controllers.

ACKNOWLEDGEMENTS

The authors would like to thank Dr. Luca Pivano from DNV GL for his valuable suggestions and discussions. Many thanks to the AMC staff for their assistance during the trials and Liam Honeychurch for his excellent workmanship of the build. Thank you also to Alex Cameron and Dr Francis Valentinis from DST Group for their help during the trials.

REFERENCES

[1] E. Ruth, Ø. N. Smogeli, T. Perez, and A. J. Sørensen, "Antispin thrust allocation for marine vessels," *IEEE Transactions on Control Systems Technology*, vol. 17, no. 6, pp. 1257–1269, Nov. 2009.

[2] L. Pivano, T. A. Johansen, and Ø. N. Smogeli, "A Four-Quadrant Thrust Estimation Scheme for Marine Propellers: Theory and Experiments," *IEEE Transactions on Control Systems Technology*, vol. 17, no. 1, pp. 215-226, Jan. 2009.

[3] M. Blanke, K. P. Lindegaard, and T. I. Fossen, "Dynamic model for thrust generation of marine propellers," *5th IFAC Conference on Manoeuvring and Control of Marine Craft*, Aalborg, Denmark, 2000, pp. 363–368.

[4] J. Carlton, *Marine Propellers and Propulsion*, 3rd ed. UK: Butterworth-Heinemann, 2012.

[5] J. Dang, J. Brouwer, R. Bosman, and C. Pouw, "Quasi-Steady Two-Quadrant Open Water Tests for the Wageningen Propeller C-and D-Series," *Twenty-Ninth Symposium on Naval Hydrodynamics*, Gothenburg, Sweden, 2012, pp. 1–19.

[6] A. Vali, B. Saranjam, and R. Kamali, "Experimental and numerical study of a submarine and propeller behaviors in submergence and surface conditions," *Journal of Applied Fluid Mechanics*, vol. 11, no. 5, pp. 1297–1308, Sep. 2018.

[7] M. Tran, J. Binns, S. Chai, A. L. Forrest, and H. Nguyen, "A practical approach to the dynamic modelling of an underwater vehicle propeller in all four quadrants of operation," *Proc IMechE Part M: J Engineering for the Maritime Environment*, vol. 233, no. 1, pp. 333–344, Feb. 2019.

[8] M. Renilson, *Submarine Hydrodynamics*, 2nd ed. USA: Springer International Publishing, 2018.

[9] D. Norrison, W. Sidebottom, and B. Anderson, "Numerical Study of a Self-Propelled Conventional Submarine," *31st Symposium on Naval Hydrodynamics*, Monterey, CA, USA, 2016, pp. 1-20.

[10] D. B. Clarke, D. Butler, C. L. Ellis, R. T. Delaney, M. Popko, and P. A. Brandner, "Propeller Dynamometer Commissioning," DST Group, Australia, Technical Note TN-1777, 2018.

[11] P. N. Joubert, “Some Aspects of Submarine Design Part 2. Shape of a Submarine 2026,” Defence Science and Technology Organisation, Australia, Technical Report TR-1920, 2006.

[12] B. Overpelt, B. Nienhuis, and B. Anderson, “Free Running Manoeuvring Model Tests On A Modern Generic SSK Class Submarine (BB2),” *Pacific International Maritime Conference*, Sydney, Australia, 2015, pp. 1-14.

[13] C. Kumar, Z. Q. Leong, D. Ranmuthugala, J. Binns, C. Carl, J. Davison, L. Hentschel, M. Courdier, and J. Duffy, “Boundary layer tripping study on a Generic Submarine Model in Water,” *21st Australasian Fluid Mechanics Conference*, Adelaide, Australia, 2018, pp. 1-4.

[14] F. R. Hama, J. D. Long, and J. C. Hegarty, “On Transition from Laminar to Turbulent Flow,” *Journal of Applied Physics*, vol. 28, no. 4, pp. 388-394, 1957.

[15] R. Burcher and L. J. Rydill, *Concepts in Submarine Design*, UK: Cambridge University Press, 1994.

[16] A. S. T. Conway, F. Valentinis, and G. Seil, “Characterisation of suction effects on a submarine body operating near the free surface,” *21st Australasian Fluid Mechanics Conference*, Adelaide, Australia, 2018, pp. 1-4.

[17] ITTC, “Terminology and Nomenclature for Propeller Geometry,” Denmark, Recommended Procedures and Guidelines 7.5-01-02-01, 2008.